Polyhedron 31 (2012) 339–344

Contents lists available at SciVerse ScienceDirect

Polyhedron

journal homepage: www.elsevier.com/locate/poly

Metal complexes of 2-aza-2-benzyl-5,10,15,20-tetraphenyl-21-carbaporphyrin: M(2-$NCH_2C_6H_5$NCTPP) (M = Ni^{2+}, Pd^{2+}) and Mn(2-$NCH_2C_6H_5$NCTPP)Br (NCTPP = N-confused 5,10,15,20-tetraphenyl porphyrinate)

De-Zhi Hsaio [a], Jyh-Horung Chen [a,*], Shin-Shin Wang [b], Jo-Yu Tung [c,*]

[a] Department of Chemistry, National Chung Hsing University, Taichung 40227, Taiwan
[b] Material and Chemical Research Laboratories, ITRI, Hsin-Chu 300, Taiwan
[c] Department of Occupational Safety and Health, Chung Hwai University of Medical Technology, Tainan 717, Taiwan

ARTICLE INFO

Article history:
Received 4 August 2011
Accepted 21 September 2011
Available online 7 October 2011

Keywords:
X-ray diffraction
Manganese(III) N-confused porphyrin
Palladium(II) N-confused porphyrin
SQUID

ABSTRACT

The crystal structures of (2-aza-2-benzyl-5,10,15,20-tetraphenyl-21-carbaporphyrinato-N,N′,N″) nickel(II) methylene chloride solvate [Ni(2-$NCH_2C_6H_5$NCTPP); **4**], (2-aza-2-benzyl-5,10,15,20-tetraphenyl-21-carbaporphyrinato-N,N′,N″) palladium(II) [Pd(2-$NCH_2C_6H_5$NCTPP); **5**] and bromo(2-aza-2-benzyl-5,10,15,20-tetraphenyl-21-carbaporphyrinato-N,N′,N″) manganese(III) toluene solvate [Mn(2-$NCH_2C_6H_5$NCTPP)Br·$C_6H_5CH_3$; **3**·$C_6H_5CH_3$] have been established. The coordination sphere around the Ni^{2+} ion in **4** (or Pd^{2+} ion in **5**) is distorted square planar (DSP), whereas for Mn^{3+} in **3**·$C_6H_5CH_3$, it is a square-based pyramid with the Br atom lying in the axial site. The *g* value of 11.34, measured from parallel polarization of the X-band EPR spectra at 4 K, is consistent with a high spin mononuclear manganese(III) centre ($S = 2$) in **3**. The magnitude of the axial (D) zero-field splitting (ZFS) for the mononuclear Mn(III) centre in **3** was determined approximately to be 1.4 cm^{-1} by paramagnetic susceptibility measurements and conventional EPR spectroscopy.

© 2011 Elsevier Ltd. All rights reserved.

1. Introduction

An N-confused porphyrin NCP is a porphyrin isomer with an inverted pyrrole ring. There are three main reaction sites in the confused pyrrole ring, i.e. 2-N, 21-C and 3-C [1]. At the external nitrogen of NCP(2-N), an electrophilic reaction can take place yielding alkylated products [1,2]. Ziegler and co-workers reported the synthesis of the 2-N-allyl-5,10,15,20-tetraphenyl N-confused porphyrin 2-NC_3H_5NCTPPH (**1**) [3]. Here in this study, the allyl group of **1** is modified to a bulky benzyl (Bz) group to derive the free base 2-N-benzyl-5,10,15,20-tetraphenyl N-confused porphyrin, 2-$NCH_2C_6H_5$NCTPPH (**2**). Unlike the NH tautomerism that exists in $NCTPPH_2$ [4], the free base **2** has only one stable form. The N-confused porphyrin **2** can provide N_3 or N_3C coordinated sites.

The shortfall in the study on metal complexes of ligand **2** prompted us to undertake the synthesis and structural investigations of its nickel(II), palladium(II) and manganese(III) complexes. In this paper, we describe the X-ray structural investigation of the metallation of **2**, leading to the nickel complex (2-aza-2-benzyl-5,10,15,20-tetraphenyl-21-carbaporphyrinato-N,N′,N″) nickel(II) [Ni(2-$NCH_2C_6H_5$NCTPP); **4**], the palladium complex (2-aza-2-benzyl-5,10,15,20-tetraphenyl-21-carbaporphyrinato-N,N′,N″) palladium(II) [Pd(2-$NCH_2C_6H_5$NCTPP); **5**] and the manganese(III) complex bromo(2-aza-2-benzyl-5,10,15,20-tetraphenyl-21-carbaporphyrinato-N,N′,N″) manganese(III) toluene solvate [Mn(2-$NCH_2C_6H_5$NCTPP)Br·$C_6H_5CH_3$; **3**·$C_6H_5CH_3$] (Scheme 1). The bulky benzyl group in this system enhances the crystallization of complexes **4**, **5** and **6**. The new diamagnetic compound **4** is used as a diamagnetic correction for the paramagnetic complex **3** in the solid-state magnetic susceptibility measurements [5]. In this paper, we also focus on the details of the electronic structure of the manganese(III) centre of **3**. Studies of the temperature dependence of the magnetic susceptibility and of the effective moment show that $S = 2$ is the ground state for the high-spin mononuclear Mn^{3+} centre in **3** at 20 °C. Application of the Bleaney–Bowers equation permits evaluation of D and an average g value for powder samples of **3** [6].

2. Experimental

2.1. Preparation of 3

The preparation of the free base 2-$NCH_2C_6H_5$NCTPPH (**2**) is shown in the Supplementary material [7]. A mixture of **2** (0.050 g, 0.071 mmol) and $MnBr_2$ (0.06 g, 0.28 mmol) were

* Corresponding authors. Tel.: +88 64 228 40411x612; fax: +88 64 228 62547 (J.-H. Chen), tel.: +88 66 267 4567x815; fax: +88 66 289 4028 (J.-Y. Tung).
E-mail addresses: JyhHChen@dragon.nchu.edu.tw (J.-H. Chen), joyuting@mail.hwai.edu.tw (J.-Y. Tung).

0277-5387/$ - see front matter © 2011 Elsevier Ltd. All rights reserved.
doi:10.1016/j.poly.2011.09.034

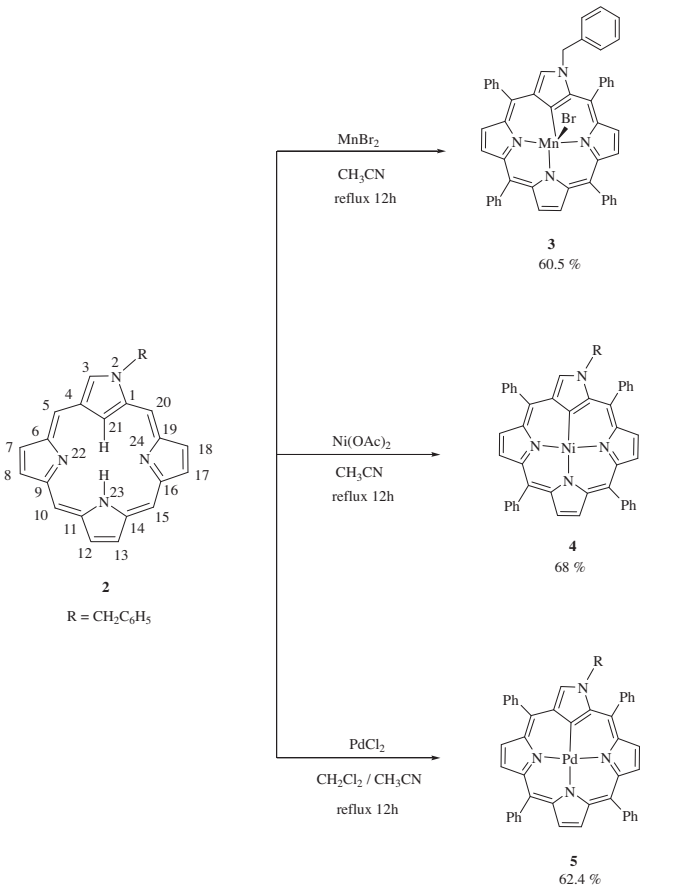

Scheme 1.

refluxed in CH_3CN (3 ml) for 12 h. After concentrating the reaction mixture, the residue was dissolved in CH_2Cl_2 (30 ml) and filtered. The filtrate was concentrated and the residue was purified over a silica gel column (230–400 mesh, 50 g) using CH_2Cl_2/EtOAc [9:1 (v/v)] as the eluent to yield a red solution of **3**. Removal of the solvent gave **3** as a green solid (0.038 g, 0.043 mmol, 60.5%). Compound **3** was dissolved in toluene and layered with hexane to afford green crystals for single crystal X-ray analysis. *Anal.* Calc. for $C_{51}H_{34}BrMnN_4{\cdot}2.5H_2O$: C, 69.39; H, 4.45; N, 6.35. Found: C, 69.42; H, 4.19; N, 6.55%. UV–Vis spectrum, λ (nm) [$\varepsilon \times 10^{-3}$ ($M^{-1}\,cm^{-1}$)] in CH_2Cl_2: 394 (32), 458 (19), 508 (60), 582 (5.0), 640 (2.5), 748 (5.0).

2.2. Preparation of *4*

A mixture of **2** (0.050 g, 0.071 mmol) and $Ni(OAc)_2$ (0.15 g, 0.60 mmol) were refluxed in CH_3CN (5 ml) for 12 h. After concentrating the reaction mixture, the residue was dissolved in 10 ml of CH_2Cl_2 and filtered. The filtrate was concentrated and the residue was recrystallized from CH_2Cl_2–hexane [1:1 (v/v)] to afford **4** (0.037 g, 0.048 mmol, 68%) as a purple solid. Compound **4** was redissolved in CH_2Cl_2 and layered with MeOH to afford purple crystals for single-crystal X-ray analysis. ^{1}H NMR (599.94 MHz, $CDCl_3$, 20 °C) δ: 8.38 [s, 1H, H_α(3)]; 8.05 [d, 1H, H_β, ^3J(H–H) = 4.8 Hz]; 7.93 [d, 1H, H_β, ^3J(H–H) = 4.8 Hz]; 7.91 [d, 1H, H_β, ^3J(H–H) = 4.8 Hz]; 7.84 [m, 6H, *o*-H]; 7.82 [d, 1H, H_β, ^3J(H–H) = 5.4 Hz]; 7.70 [d, 1H, H_β(17), ^3J(H–H) = 5.4 Hz]; 7.67 [d, 1H, H_β(18), ^3J(H–H) = 4.8 Hz]; 7.56 [m, 10H, *m*-, *p*-H]; 7.46 [d, 2H, *o*-H(40, 44), ^3J(H–H) = 6.6 Hz]; 7.33 [t, 1H, *m*-H(41, 43), ^3J(H–H) = 7.8 Hz]; 7.13 [t, 1H, *p*-H(49) of benzyl group, ^3J(H–H) = 7.5 Hz]; 7.07 [t, 2H, *m*-H(48, 50) of benzyl group, ^3J(H–H) = 7.5 Hz]; 6.65 [d, 2H, *o*-H(47, 51) of benzyl group, ^3J(H–H) = 7.2 Hz]; 5.11 [s, 2H, H(45) of benzyl group] (Fig. 3). *Anal.* Calc. for $C_{51}H_{34}N_4Ni{\cdot}0.2CH_2Cl_2{\cdot}2.0C_4H_8O_2$: C, 74.47; H, 5.32; N, 5.87. Found: C, 74.24; H, 5.05; N, 5.88%. UV–Vis spectrum, λ (nm) [$\varepsilon \times 10^{-3}$ ($M^{-1}\,cm^{-1}$)] in CH_2Cl_2: 428 (73), 462 (40), 508 (60), 560 (8.4), 718 (3.8).

2.3. Preparation of *5*

Compound **5** was prepared in 62.4% yield in the same way as described for **4**, but using $PdCl_2$ and **2**. Compound **5** was dissolved in CH_2Cl_2 and layered with EtOAc (ethyl acetate) to get purple crystals for single-crystal X-ray analysis. ^{1}H NMR (599.94 MHz, $CDCl_3$, 20 °C) δ: 8.31 [s, 1H, H_α(19)]; 8.02[d, 1H, H_β, ^3J(H–H) = 4.8 Hz]; 7.88 [m, 6H, *o*-H]; 7.85 [d, 1H, H_β, ^3J(H–H) = 5.4 Hz]; 7.83 [d, 1H, H_β, ^3J(H–H) = 4.8 Hz]; 7.78 [d, 1H, H_β, ^3J(H–H) = 4.8 Hz]; 7.72 [d, 1H, H_β, ^3J(H–H) = 4.8 Hz]; 7.58 [d, 1H, H_β, ^3J(H–H) = 4.2 Hz]; 7.56 [m, 10H, *m*-, *p*-H]; 7.51 [d, 2H, *o*-H(34, 38), ^3J(H–H) = 7.2 Hz]; 7.34 [t, 1H, *m*-H(35, 37), ^3J(H–H) = 7.8 Hz]; 7.12 [t, 1H, *p*-H(49) of benzyl group, ^3J(H–H) = 6.9 Hz]; 7.06 [t, 2H, *m*-H(48, 50) of benzyl group, ^3J(H–H) = 7.5 Hz]; 6.66 [d, 2H, *o*-H(47, 51) of benzyl group, ^3J(H–H) = 7.8 Hz]; 5.14 [s, 2H, H(45) of benzyl group] (Fig. S1 in Supplementary material). *Anal.* Calc. for $C_{51}H_{34}N_4Pd{\cdot}0.6H_2O{\cdot}1.6C_4H_8O_2{\cdot}0.6CH_2Cl_2$: C, 68.84; H, 4.90; N, 5.54. Found: C, 68.79; H, 5.09; N, 5.13%. UV–Vis spectrum, λ (nm) [$\varepsilon \times 10^{-3}$ ($M^{-1}\,cm^{-1}$)] in CH_2Cl_2: 430 (61), 450 (88), 532 (8.1), 576 (6.5), 638 (3.2), 696 (7.6), 764 (8.9).

2.4. Magnetic susceptibility measurements

The solid-state magnetic susceptibility was measured under helium on a Quantum Design MPMS5 SQUID susceptometer from 2 to 300 K at a field of 5 kG. The sample was held in a Kel-F bucket. The bucket had been calibrated independently at the same field and temperature. The raw data for **3** was corrected for the molecular diamagnetism. The diamagnetic contribution of the sample was measured from the analogous diamagnetic metal complex, **4**. Details of the diamagnetic corrections that were made can be found in Ref. [5].

2.5. Spectroscopy

ESR spectra were measured on an X-band Bruker EMX-10 spectrometer equipped with an Oxford Instruments liquid helium cryostat. Magnetic field values were measured with a digital counter. The X-band resonator was a dual-mode cavity (Bruker ER 4116 DM). Proton NMR spectra were recorded at 599.95 MHz on a Varian Unity Inova-600 spectrometer locked on deuterated solvent and referenced to the solvent peak. Proton NMR is relative to $CDCl_3$ at δ = 7.24. The mass spectra [MS(ESI)] were recorded on a Finnigan TSQ Ultra EMR mass spectrometer with an ESI source. UV–Vis spectra were recorded at 20 °C on a Hitachi U-3210 spectrophotometer.

2.6. Crystallography

Table 1 presents the crystal data as well as other information for **3**, **4** and **5**. Measurements were taken on a Bruker AXS SMART-1000 diffractometer using monochromatized Mo Kα radiation (λ = 0.71073 Å). Semi-empirical absorption corrections were made for the three complexes. The structures were solved by direct methods (SHELXTL-97) [8] and refined by the full-matrix least-squares method. All non-hydrogen atoms were refined with anisotropic thermal parameters, whereas all hydrogen atoms were placed in calculated positions and refined with a riding model. We have used SQUEEZE to remove the disordered solvent CH_2Cl_2

Table 1
Crystal data for **3**·$C_6H_5CH_3$, **4** and **5**.

Compound	**3**·$C_6H_5CH_3$	**4**	**5**
Empirical formula	$C_{58}H_{42}N_4BrMnN_4$	$C_{51}H_{34}N_4Ni$	$C_{51}H_{34}N_4Pd$
Formula weight	929.81	761.53	809.22
Space group	$P2_1/n$	$P\bar{1}$	$P\bar{1}$
Crystal system	monoclinic	triclinic	triclinic
a (Å)	10.3156(3)	11.8610(4)	11.8973(5)
b (Å)	15.9025(5)	13.3696(3)	13.4226(5)
c (Å)	26.929 (1)	13.7129(4)	13.5182(6)
α (°)	90	102.924(2)	102.531(3)
β (°)	97.827(4)	109.836(3)	108.893(4)
γ (°)	90	91.199(2)	92.037(3)
V (Å^3)	4376.4(3)	1982.6(1)	1980.7(1)
Z	4	2	2
F(000)	1912	792	828
D_{calc} (g cm^{-3})	1.411	1.276	1.357
λ(Mo Kα) (mm^{-1})	1.261	0.530	0.510
S	1.057	1.081	1.066
Crystal size (mm)	0.34 × 0.32 × 0.26	0.60 × 0.22 × 0.08	0.46 × 0.32 × 0.24
θ (°)	2.82–29.12	2.54–29.25	2.84–29.23
T (K)	110(2)	120(2)	110(2)
Number of reflections measured	10038	9052	9137
Number of reflections observed	5184	6338	6951
R_1[a]	0.0769	0.0462	0.0413
wR_2[b]	0.2209	0.1175	0.1111

[a] $R_1 = [\sum||F_o| - |F_c||/\sum|F_o|]$.
[b] $wR_2 = [\sum w(F_o^2 - F_c^2)^2/\sum w(F_o^2)^2]^{1/2}$.

Table 2
Selected bond distances (Å) and angles (°) for compounds **3**·$C_6H_5CH_3$, **4** and **5**.

3·$C_6H_5CH_3$			
Bond lengths (Å)			
Mn–N(1)	2.036(4)	Mn–C(17)	2.007(5)
Mn–N(2)	2.047(4)	Mn–Br	2.487(1)
Mn–N(3)	2.035(4)		
Bond angles (°)			
Br–Mn–N(1)	104.8(1)	C(17)–Mn–N(1)	87.6 (2)
Br–Mn–N(2)	97.3 (1)	C(17)–Mn–N(2)	159.8(2)
Br–Mn–N(3)	93.6 (1)	C(17)–Mn–N(3)	87.3(2)
Br–Mn–C(17)	102.9(1)	N(1)–Mn–N(2)	88.3(2)
N(2)–Mn–N(3)	90.4 (2)	N(1)–Mn–N(3)	161.6(2)
4			
Bond lengths (Å)			
Ni–N(1)	1.957(2)	Ni–N(3)	1.940 (2)
Ni–N(2)	1.968(2)	Ni–C(2)	1.907(2)
Bond angles (°)			
N(1)–Ni–N(2)	90.37(8)	N(1)–Ni–C(2)	89.38(9)
N(1)–Ni–N(3)	178.47(9)	N(2)–Ni–C(2)	178.3(1)
N(2)–Ni–N(3)	90.62(8)	N(3)–Ni–C(2)	89.67(9)
5			
Bond lengths (Å)			
Pd–N(1)	2.027(2)	Pd–N(3)	2.014(2)
Pd–N(2)	2.053(2)	Pd–C(17)	1.973(3)
Bond angles (°)			
N(1)–Pd–N(2)	90.10(9)	N(1)–Pd–C(17)	89.64(1)
N(1)–Pd–N(3)	178.4 (1)	N(2)–Pd–C(17)	178.4(1)
N(2)–Pd–N(3)	90.7(1)	N(3)–Pd–C(17)	89.6(1)

for the Ni structure (**4**). Table 2 lists selected bond distances and angles for the three complexes.

3. Results and discussion

3.1. Structures of 3·$C_6H_5CH_3$, 4 and 5

The complexes Ni(2-$NCH_2C_6H_5$NCTPP) (**4**) and Pd(2-$NCH_2C_6H_5$NCTPP) (**5**) were synthesized in 68% and 62.4% yields, respectively, by reacting **2** with excess $Ni(OAc)_2$ or $PdCl_2$ in CH_3CN or CH_2Cl_2/CH_3CN under aerobic conditions (Scheme 1).

The complex Mn(2-$NCH_2C_6H_5$NCTPP)Br (**3**) was produced in 60.5% yield by heating a solution of **2** in CH_3CN under aerobic conditions with an excess of $MnBr_2$ (Scheme 1).

The X-ray frameworks for **3**·$C_6H_5CH_3$, **4** and **5** are depicted in Fig. 1. All these structures, distorted square planar (DSP) for the nickel centre of **4** (or palladium centre of **5**) and five-coordinate manganese centre of **3**·$C_6H_5CH_3$, bond with three nitrogen atoms (N_3) of the porphyrin and one carbon atom (C) of the inverted pyrrole ring in common, whilst compound **3**·$C_6H_5CH_3$ has an addition Br ligand in the axial site.

The distortion in the five-coordinate complex **3**·$C_6H_5CH_3$ can be quantified by the "degree of trigonality" which is defined as $\tau = (\beta - \alpha)/60$, where β is the largest and α the second largest of the L_{basal}–M–L_{basal} angles [9]. The limiting values are $\tau = 0$ for an ideal tetragonal geometry and $\tau = 1$ for an ideal trigonal bipyramid geometry. In the present case, we find $\beta = 161.6(2)°$ [N(1)–Mn–N(3)] and $\alpha = 159.8(2)$ [C(17)–Mn–N(2)]. Thus the τ value calculated for **3**·$C_6H_5CH_3$ is 0.03. Hence the geometry around Mn(III) in **3**·$C_6H_5CH_3$ is best described as a square-based pyramid in which the apical site is occupied by the Br atom. The Mn–C(17), Mn–N(1), Mn–N(2), Mn–N(3) and Mn–Br bond lengths in **3**·$C_6H_5CH_3$ are 2.007(5), 2.036(4), 2.047(4), 2.035(4) and 2.487(1) Å, respectively. The crystal packing of complex **3** is shown in Fig. 2. The short inter atomic contacts of H(45B)...BrA, 2.964(4) Å, for **3** is much longer than that of H(39B)...BrBA, 2.800(5) Å [or H(45B)...BrC, 2.846(4) Å] in Mn(2-NC_3H_5NCTPP)Br [or Mn(2-NCH_2-*p*-C_6H_4-CO_2CH_3NCTPP)Br] [10].[1] Hence there are no intermolecular hydrogen bonds linking the individual monomer of **3** into a dimer in the solid state. Complex **3** is monomeric in the solid phase.

In **4** (or **5**), the geometry about Ni (or Pd) is distorted square-planar and the bond distances are as follows: Ni–C(2) = 1.907(2), Ni–N(1) = 1.957(2), Ni–N(2) = 1.968(2) and Ni–N(3) = 1.940(2) Å for **4**; Pd–C(17) = 1.973(3), Pd–N(1) = 2.027(2), Pd–N(2) = 2.053(2) and Pd–N(3) = 2.014(2) Å for **5**. The average Ni–N distance of 1.955(2) in **4** is comparable to the Ni–N distances in the planar Ni(CTTP) derivative [1.955(3) Å, CTTP = 2-aza-21-carba-5,10,15,20-tetra-*p*-tolylporphyrinate] but the Ni–C distance of 1.907(2) Å in **4** is smaller than the Ni–C distance in the same Ni(CTTP) complex [1.963(3) Å] [11]. The average Pd–N and Pd–C distances are 2.031(2) and 1.973(3) Å in **5**, and these are both smaller than those of Pd(II)–N (2.09 Å) and Pd(II)–C (2.00 Å) in the square-planar Pd(NCTPP) [12].

3.2. ^{1}H NMR spectroscopic data for 4 and 5 in $CDCl_3$

In solution, the ^{1}H NMR spectrum exhibits six pyrrole resonances [H_β(18), H_β(17), H_β(13), H_β(12), H_β(8), H_β(7)] for **4** (Fig. 3). The doublet at 7.70 ppm is assigned as H_β(17) with ^3J(H–H) = 5.4 Hz and the other doublet at 7.67 ppm is due to H_β(18) with ^3J(H–H) = 4.8 Hz. The doublet at 8.05 ppm is assigned as H_β with ^3J(H–H) = 5.1 Hz and the other doublet at 7.82 ppm is due to H_β with ^3J(H–H) = 5.1 Hz. The doublet at 7.93 ppm is assigned as H_β with ^3J(H–H) = 4.8 Hz and the other doublet at 7.90 ppm is due

[1] Mn(2-$NCH_2CH = CH_2$NCTPP)Br = bromo(2-aza-2-allyl-5,10,15,20-tetraphenyl-21-carbaporphyrinato-N,N′,N″) manganese (III); Mn(2-NCH_2-*p*-C_6H_4-CO_2CH_3NCTPP) Br = [2-aza-2-(4′-methyl methylbenzoate)-5,10,15,20-tetraphenyl-21-carbaporphyrinato-N,N′,N″] manganese(III).

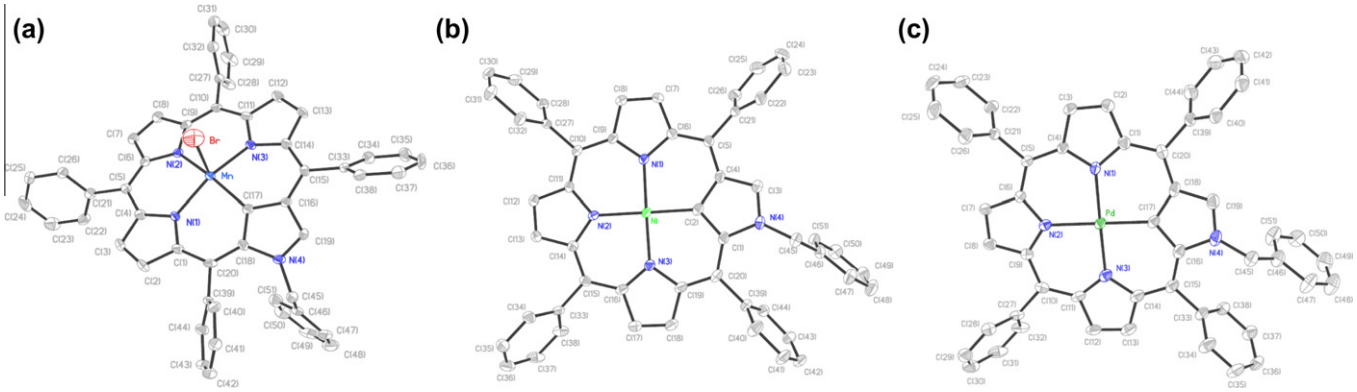

Fig. 1. Molecular structures of (a) [Mn(2-NCH$_2$C$_6$H$_5$NCTPP)Br·C$_6$H$_5$CH$_3$; **3**·C$_6$H$_5$CH$_3$]; (b) [Ni(2-NCH$_2$C$_6$H$_5$NCTPP); **4**] and (c) [Pd(2-NCH$_2$C$_6$H$_5$NCTPP); **5**], with 30% thermal ellipsoids. Hydrogen atoms are omitted for clarity.

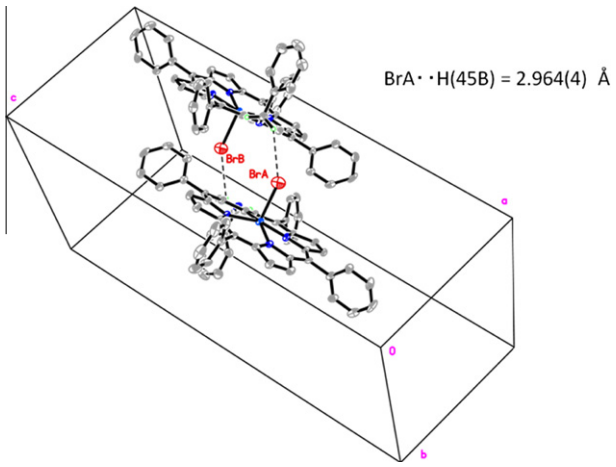

Fig. 2. The crystal packing in the unit cell for complex **3**.

to H$_\beta$ with ^3J(H–H) = 4.8 Hz. The external benzyl ligand (Bz) unit in **4** gave rise to series of ^{1}H resonances at 7.13 [t, 1H, *p*-H(49), ^3J(H–H) = 7.5 Hz], 7.07 [t, *m*-H(48, 50), ^3J(H–H) = 7.5Hz], 6.65 [d, *o*-H(47, 51), ^3J(H–H) = 7.2 Hz] and 5.11 [s, H(45)].

In solution, the ^{1}H NMR spectrum exhibits six pyrrole resonances [H$_\beta$(13), H$_\beta$(12), H$_\beta$(7), H$_\beta$(8), H$_\beta$(3), H$_\beta$(2)] for **5** (Fig. S1 in Supplementary material). The doublet at 8.02 ppm is assigned as H$_\beta$ with ^3J(H–H) = 5.1 Hz and the other doublet at 7.85 ppm is due to H$_\beta$ with ^3J(H–H) = 5.1 Hz. The doublet at 7.83 ppm is assigned as H$_\beta$ with ^3J(H–H) = 4.8 Hz and the other doublet at 7.78 ppm is due to H$_\beta$ with ^3J(H–H) = 4.8 Hz. The doublet at 7.72 ppm is assigned as H$_\beta$ with ^3J(H–H) = 4.5 Hz and the other doublet at 7.58 ppm is due to H$_\beta$ with ^3J(H–H) = 4.5 Hz. The external benzyl ligand (Bz) unit in **5** gave rise to series of ^{1}H resonances at 7.12 [t, 1H, *p*-H(49), ^3J(H–H) = 7.5 Hz], 7.06 [t, *m*-H(48, 50), ^3J(H–H) = 7.5 Hz], 6.66 [d, *o*-H(47, 51), ^3J(H–H) = 7.8 Hz] and 5.14 [s, H(45)]. The diamagnetic properties of **4** and **5** were inferred from their diamagnetic ^{1}H NMR spectra in CDCl$_3$.

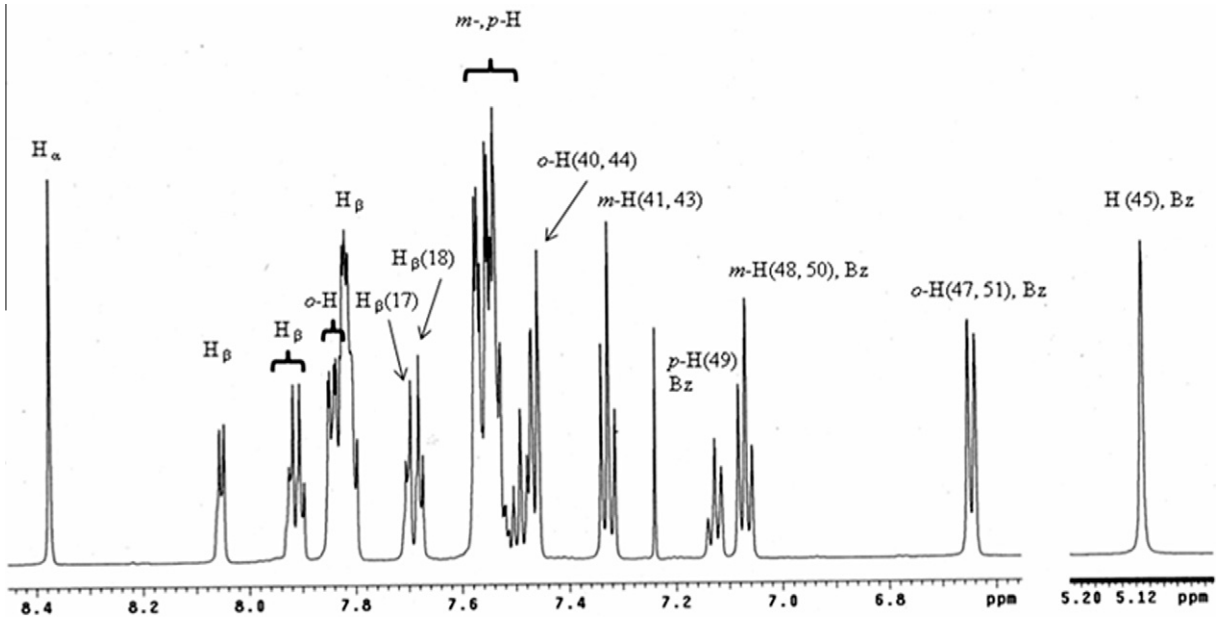

Fig. 3. ^{1}H NMR spectrum for **4** at 599.95 MHz in CDCl$_3$ at 20 °C showing six different β-pyrrole protons H$_\beta$, phenyl protons (*o*-H, *m*, *p*-H) and protons of the benzyl ligand (Bz). Chemical shifts are in ppm from CDCl$_3$ at 7.24 ppm.

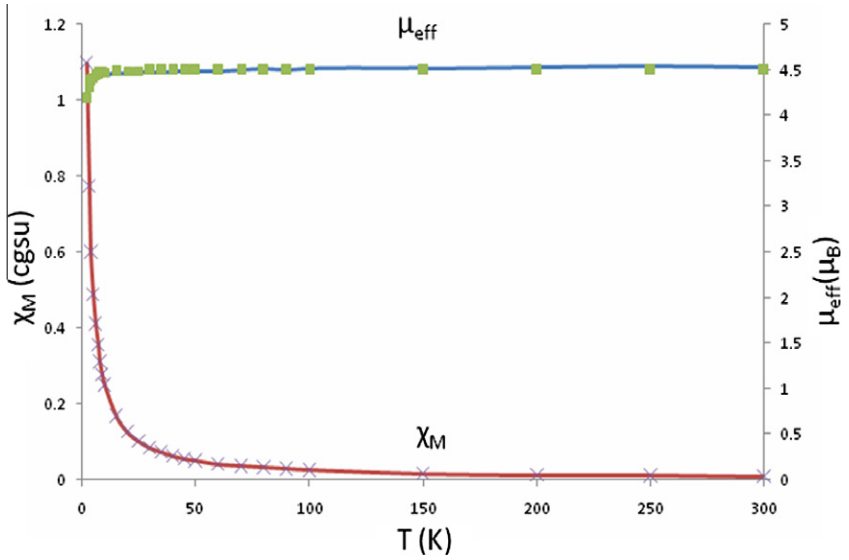

Fig. 4. Temperature variation of the molar magnetic susceptibility (χ_m) and effective magnetic moment (μ_{eff}) for a powder sample of **3** in the range 2–300 K. Points represent the experimental data; solid lines represent the least-squares fit of the data to Eq. (1).

3.3. ESR studies

The X-band (9.377 GHz) ESR spectrum using parallel polarization recorded for **3** as a powder solid at 20 °C is shown in Fig. S2 (Supplementary material). As has been similarly observed in other Mn(III) complexes, a single line, centred at $g = 11.34$, is found [13–15]. These signals are attributed to a forbidden transition within the $|2^{+}\rangle$ and $|2^{-}\rangle$ non-Kramer's doublet for a high-spin mononuclear Mn^{3+} ($S = 2$) complex [14,15].

3.4. Magnetic properties

Magnetic data for complex **3** are reported in Fig. 4 in the forms of χ_M and μ_{eff} versus T. As can be seen in Fig. 4, the value of μ_{eff} varies from 4.53 μ_B at 300 K to 4.18 μ_B at 2 K. The magnetic moment clearly shows a plateau equal to 4.50 μ_B at high temperatures (300–15 K), below which it decreases again. The abrupt rise in μ_{eff} in the range $2 < T < 15$ K is characteristic of a compound with significant zero-field splitting (ZFS). The room-temperature effective moment of 4.53 μ_B is lower than the spin-only moment of 4.9 μ_B for an $S = 2$ system, but consistent with that of other high-spin Mn(III) complexes in which $g < 2$. The χ_M versus T (or μ_{eff} versus T) data could fit into the expression (Eq. (1)) derived from the Hamiltonian $\hat{H} = D[S_z^2 - \frac{1}{3}S(S+1)] + E(S_x^2 - S_y^2) + g\mu_B HS$, where H is the applied magnetic field, g is the g tensor, $S = 2$ is the electronic spin, and D and E are the parameters which describe the effects of axial and rhombic ligand fields, respectively [16]. As a first approximation, we set $E = 0$ in **3**. The data were inserted into the Bleaney–Bowers equation (Eq. (1)) [6]

$$\bar{\chi}_M = \frac{0.3749}{T} g^2 \left\{ p \cdot \frac{1}{3} \overbrace{\left[\frac{8 + 2e^{3y} + \frac{1}{y}(-\frac{8}{3} - \frac{28}{3}e^{3y} + 12e^{4y})}{2 + 2e^{3y} + e^{4y}} \right]}^{Mn^{3+}} + \underbrace{(1-p) \times 2.917}_{Mn^{2+}\,(impurity)} \right\} + TIP \qquad (1)$$

where $y = 1.44 \frac{D(cm^{-1})}{T}$ and $\mu_{eff} = 2.828\sqrt{\chi_M T}$.

Here g is the average g value, TIP is the temperature independent paramagnetism, p is the fraction of Mn^{3+}, and other symbols have their standard meanings. The best fits, as represented in Fig. 4, gave the values $g = 1.84$, $|D| = 1.4$ cm^{-1}, $p = 0.9999$ and TIP = -1.1×10^{-4} (cm^3/mol). This $|D|$ value lies in the $1 < |D| < 4.9$ cm^{-1} range found in related Mn(III) porphyrin complexes.

4. Conclusion

We have investigated three new inverted N-confused porphyrin metal complexes, namely paramagnetic **3** and two diamagnetic complexes **4** and **5**, and their X-ray structures were established. The conventional ESR spectroscopy and the magnetic susceptibility measurements were reported to evaluate the ZFS parameter D for the high-spin mononuclear Mn(III) ($S = 2$) complex **3**.

Acknowledgements

Financial support from the National Science Council of the R.O.C. under Grants NSC 99-2113-M-005-006 and 99-2119-M-273-001 is gratefully acknowledged. We thank Dr. S. Elango for helpful discussions.

Appendix A. Supplementary data

The preparation of **2** is shown in the Supplementary material. CCDC 834007, 834008 and 834009 contains the supplementary crystallographic data for **3**, **4** and **5**, respectively. These data can be obtained free of charge via http://www.ccdc.cam.ac.uk/conts/retrieving.html, or from the Cambridge Crystallographic Data Centre, 12 Union Road, Cambridge CB2 1EZ, UK; fax: (+44) 1223-336-033; or e-mail: deposit@ccdc.cam.ac.uk. Supplementary data associated with this article can be found, in the online version, at doi:10.1016/j.poly.2011.09.034.

References

[1] X. Li, B. Liu, P. Yi, R. Yi, X. Yu, P.J. Chimelewski, J. Org. Chem. 76 (2011) 2345.
[2] T. Ishizuka, H. Yamasaki, A. Osuka, H. Furuta, Tetrahedron Lett. 63 (2007) 5137.
[3] W. Qu, T. Ding, A. Cetin, J.D. Harvey, M.J. Taschner, C.J. Ziegler, J. Org. Chem. 71 (2006) 811.
[4] P.J. Chimelewski, L. Latos-Grazynski, J. Chem. Soc., Perkin Trans. 2 (1995) 503.
[5] R.S. Drago, Physical Methods for Chemists, second ed., Sanders College Publishing, New York, 1992. p. 473, 591.
[6] B. Bleaney, K.D. Bowers, Proc. R. Soc. Lond. A214 (1952) 451.
[7] D.Z. Hsaio, J.H. Chen, S.S. Wang, J.Y Tung, Polyhedron 30 (2011) 2908.

[8] G.M. Sheldrick, SHELXL-97, Program for the Refinement of Crystal structure from Diffraction Data, University of Gottingen, Gottingen, Germany, 1997.
[9] A.W. Addison, T.N. Rao, J. Reedijk, J.V. Rijn, G.C. Verschoor, J. Chem. Soc., Dalton Trans. (1984) 1349.
[10] C. Yang, M.Y. Tsai, S.W. Hung, J.H. Chen, S.S. Wang, J.Y. Tung, personal communication.
[11] P.J. Chmielewski, L. Lato-Grazynski, K. Rachlewicz, T. Glowiak, Angew. Chem., Int. Ed. 33 (1994) 779.
[12] H. Furuta, N. Kubo, H. Maeda, T. Ishizuka, A. Osuka, H. Nanami, T. Ogawa, Inorg. Chem. 39 (2000) 5424.
[13] E.P. Talsi, K.P. Bryliakov, Mendeleev Commun. (2004) 111.
[14] S.L. Dexheimer, J.W. Gohdes, M.K. Chan, K.S. Hagen, W.H. Armstrong, M.P. Klein, J. Am. Chem. Soc. 111 (1989) 8923.
[15] K.P. Bryliakov, D.E. Babushkon, E.P. Talsi, Mendeleev Commun. (1999) 29.
[16] S.W. Hung, F.A. Yang, J.H. Chen, S.S. Wang, J.Y. Tung, Inorg. Chem. 47 (2008) 7202.